Collisional Excitation of PO^+ by para-H_2

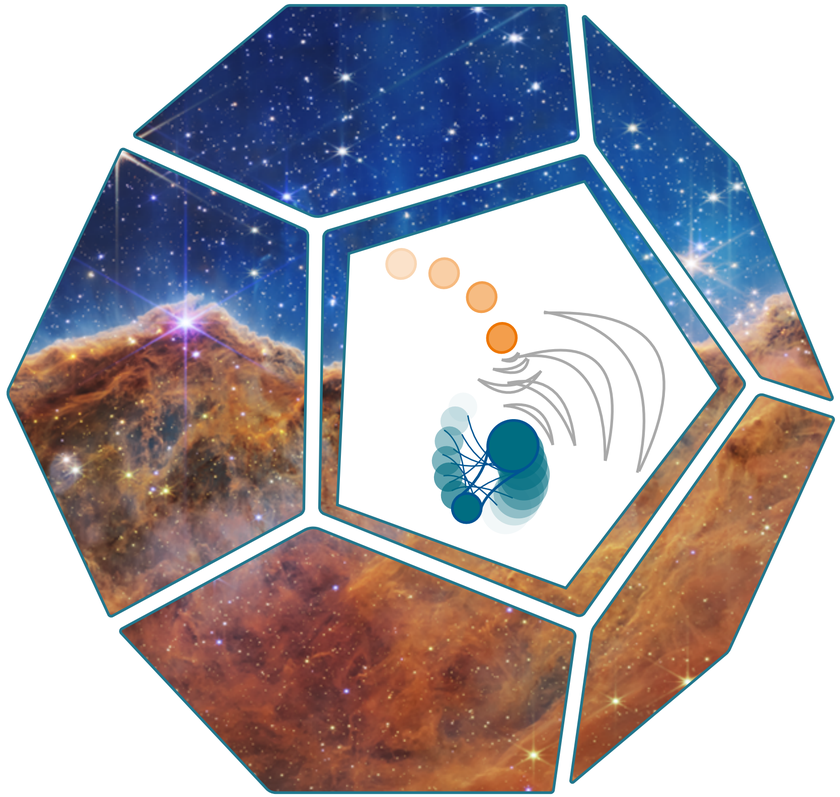

Towards the Accurate Modeling of Phosphorus Abundance in the ISM

PCMI2024-Bordeaux
Colloque du Programme Physique Chimie du Milieu Interstellaire

Francesca Tonolo

COLLEXISM

European Research Council
Established by the European Commission

PO+ and H_2 system

Why Ions?

The ionization degree is a **diagnostic** tool of the **evolutionary stage** of astrophysical objects.

Ions play a prominent role in **chemical reactivity**.

$$x(e^-) = n(e^-)/n(\mathrm{H_2})$$

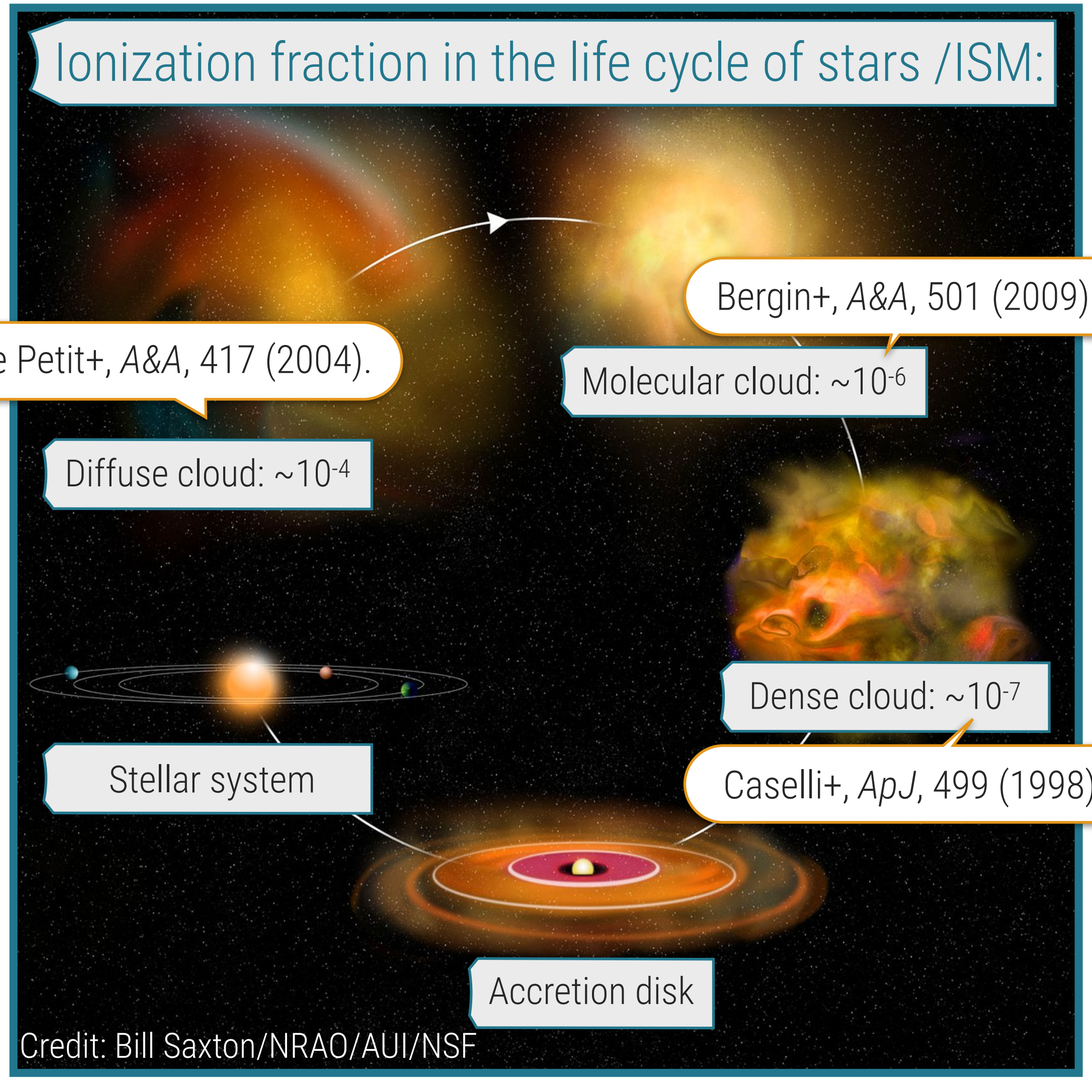

PO^+ and H_2 system

Why Phosphorus?

B. K. Pearce+, *Proc. Natl. Acad. Sci*, **114**, (2017).

Element of pivotal importance from a **prebiotic** point of view. It is ubiquitous in our planet and P-bearing compounds have been found also in many environments outside Earth.

However, only **few** a P-bearing molecules have been **identified in the ISM**:

- **Depletion** onto interstellar grains;
- **Paucity** of **observational data** and chemical modeling studies.

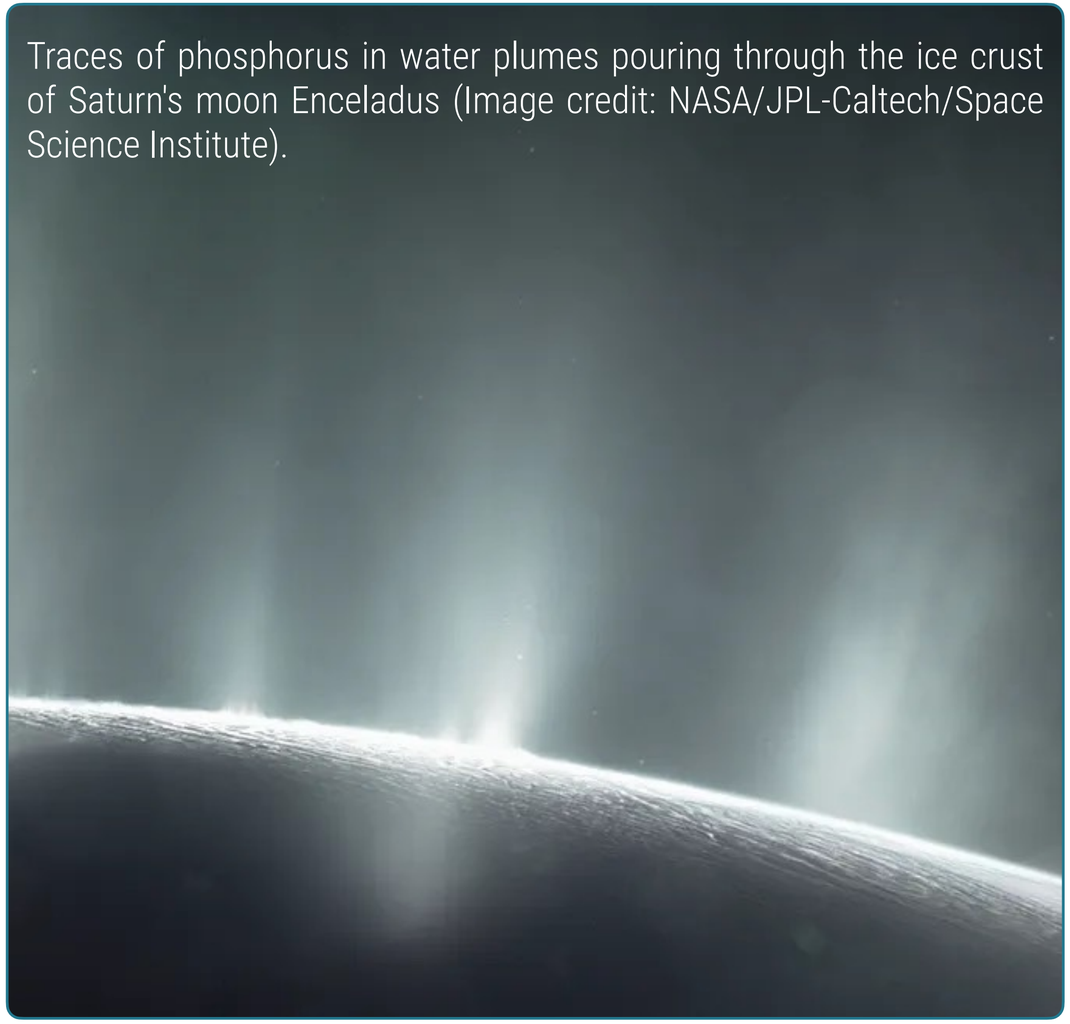

Traces of phosphorus in water plumes pouring through the ice crust of Saturn's moon Enceladus (Image credit: NASA/JPL-Caltech/Space Science Institute).

PO+ and H_2 system

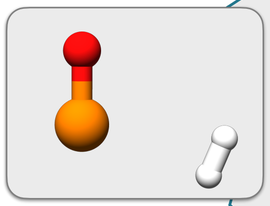

Target species: **PO+** recently detected in the **molecular cloud G+0.693-0.02** where, due to the low density of H_2, **LTE condition is not achieved.**

Collider: in ISM, the most abundant perturber is **H_2**.

V. M. Rivilla, et al. (2022), *FSPAS*, **9**, 829288.

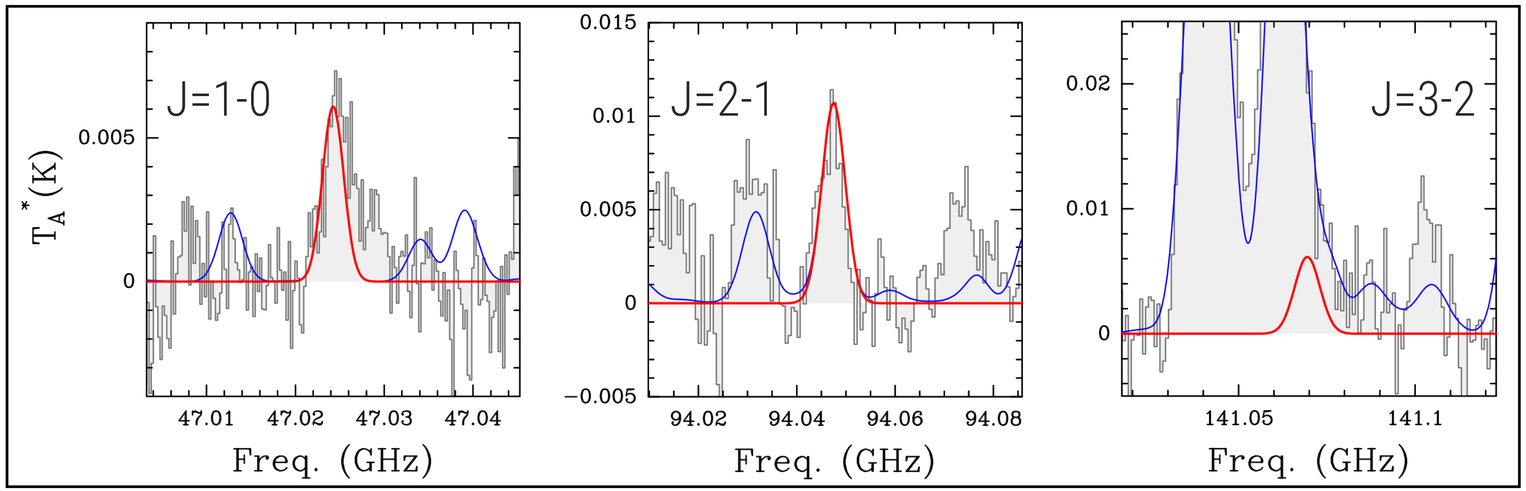

G+0.693-0.027 molecular cloud:

- Very low densities of H_2 ($\sim 1 \times 10^4$ cm^{-3});
- High kinetic temperatures (~ 150 K);

S. Zeng, et al. (2018), *MNRAS*, **478**, 2962;
S. Zeng, et al. (2020), *MNRAS*, **497**, 4896.

Intermolecular PES

MOLPRO

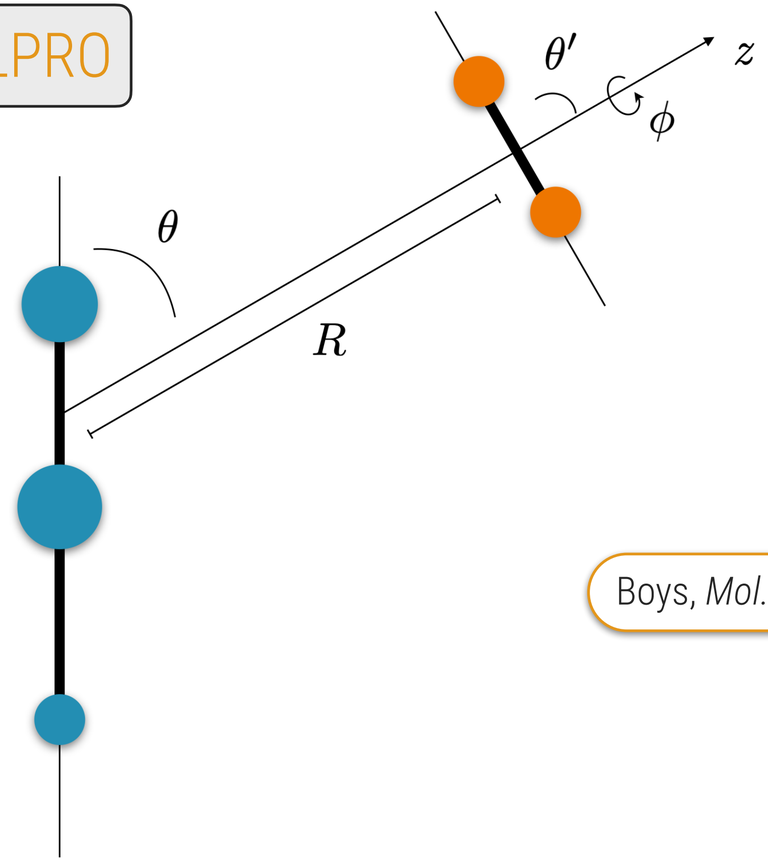

Jacobi internal coordinates of a collisional system.

Geometries:

- The two colliders are considered as **rigid bodies** and only the interaction between them is taken into account.
- The body-fixed **Jacobi coordinates** frame is employed.

Interaction energies:

- *Ab initio* calculations over an irregular grid in the $\{R, \theta, \theta', \phi\}$ coordinates.
- Each energy has been corrected for the basis set superposition error (**BSSE**).

Boys, *Mol.Phys.*, **19** (1970).

Single point energies:
CCSD(T)-F12/aug-cc-pV(Q+d)Z level of theory.

Fitting of the potential:

$$V(R,\theta,\theta',\phi) = \sum_{l_1 l_2 \mu} v_{l_1 l_2 \mu}(R)\, s_{l_1 l_2 \mu}(\theta,\theta',\phi)$$

Fitting the 4D potential

$$V(R,\theta,\theta',\phi) = \sum_{l_1 l_2 \mu} v_{l_1 l_2 \mu}(R)\, s_{l_1 l_2 \mu}(\theta,\theta',\phi)$$

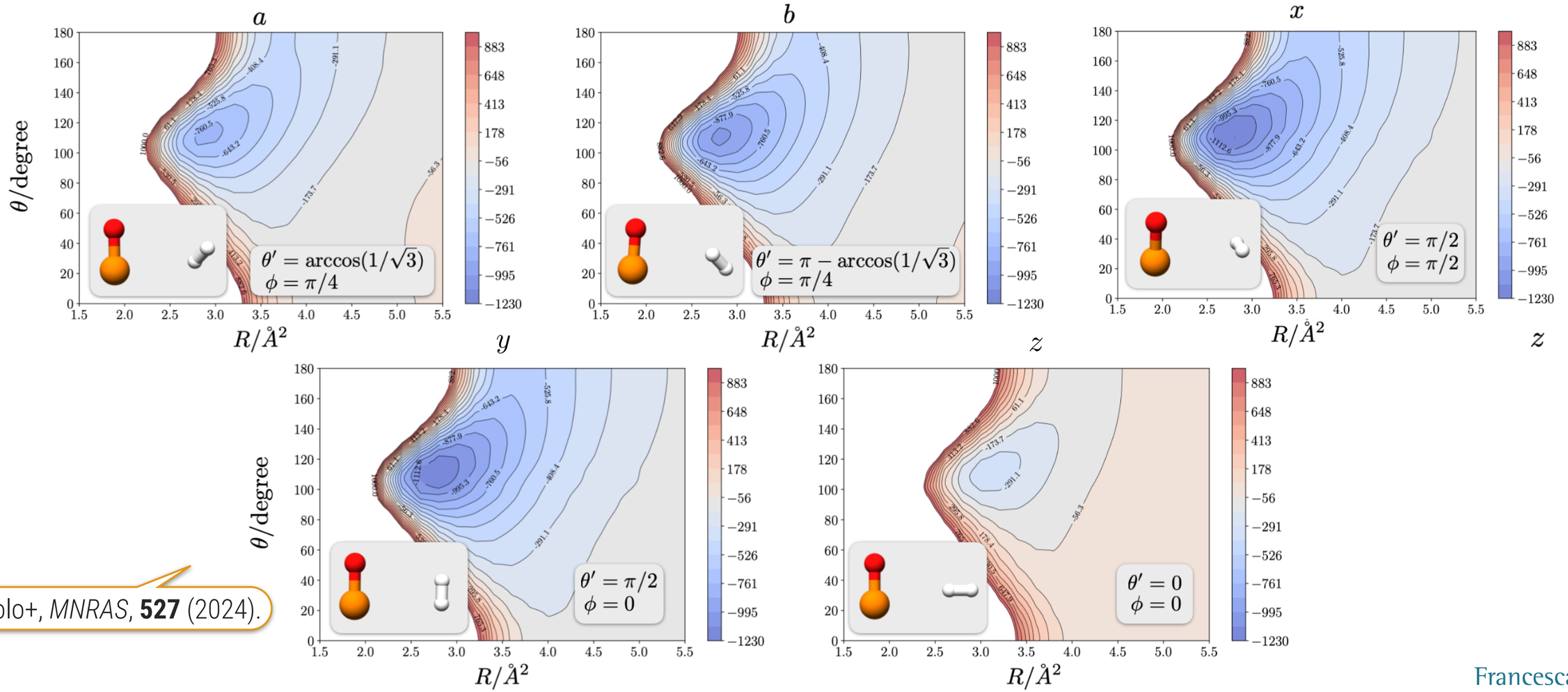

Tonolo+, *MNRAS*, **527** (2024).

Fitting the 4D potential

$$V(R,\theta,\theta',\phi) = \sum_{l_1 l_2 \mu} v_{l_1 l_2 \mu}(R)\, s_{l_1 l_2 \mu}(\theta,\theta',\phi)$$

where: $s_{l_1,l_2,\mu}(\theta,\theta',\phi) = A_{l_1}\left[< l_1 0 l_2 0 \mid l_1 l_2 \mu 0 > P_{l_1 0}(\theta) P_{l_2 0}(\theta') + \sum_m (-1)^m 2 \left\langle l_1 m l_2 - m \mid l_1 l_2 \mu 0 \right\rangle P_{l_1 m}(\theta) P_{l_2 m}(\theta') \cos(m\phi) \right]$,

$P_{lm}(\theta) = Y_{lm}(\theta,\phi)\exp(-\mathrm{i}m\phi)$.

Truncation of the expansion at the $l_2 < 2$ terms of the angular momentum of the collider:

The only basis function describing the dependence of the potential on the relative orientations of the collider are $Y_{00}, Y_{20}, Y_{21}, Y_{22}$.

↓

Reliable choice of **five sets** of $\{\theta', \phi\}$ coordinates to describe the system:

$$V(R,\theta,\theta',\phi) = V_{iso} + \frac{1}{2}\left[V_{eff}(z) - V_{iso}\right]\left(3\cos^2\theta'\right) + \frac{3}{2}\left[V_{eff}(a) - V_{eff}(b)\right]\sin\theta'\cos\theta'\cos\phi + \frac{1}{2}\left[V_{eff}(x) - V_{eff}(y)\right]\sin^2\theta'\cos(2\phi)$$

Spherical average approximation

If the **inclusion of the rotational structure** ($j \neq 0$) of the collider has a negligible effect on the cross sections' values, a spherical average of the potential with respect to five orientations of the collider can be performed:

$$V_{\mathrm{av}}(R,\theta) = \sum_{l_1} v_{l_1}(R) P_{l_1}(\cos(\theta)),$$

$$V_{\mathrm{av}}(R,\theta) = \frac{1}{7}[2(V(R,\theta,a) + V(R,\theta,b)) + (V(R,\theta,x) + V(R,\theta,y) + V(R,\theta,z))]\,.$$

The collider is considered as a **structureless species**, behaving as a rotating sphere.

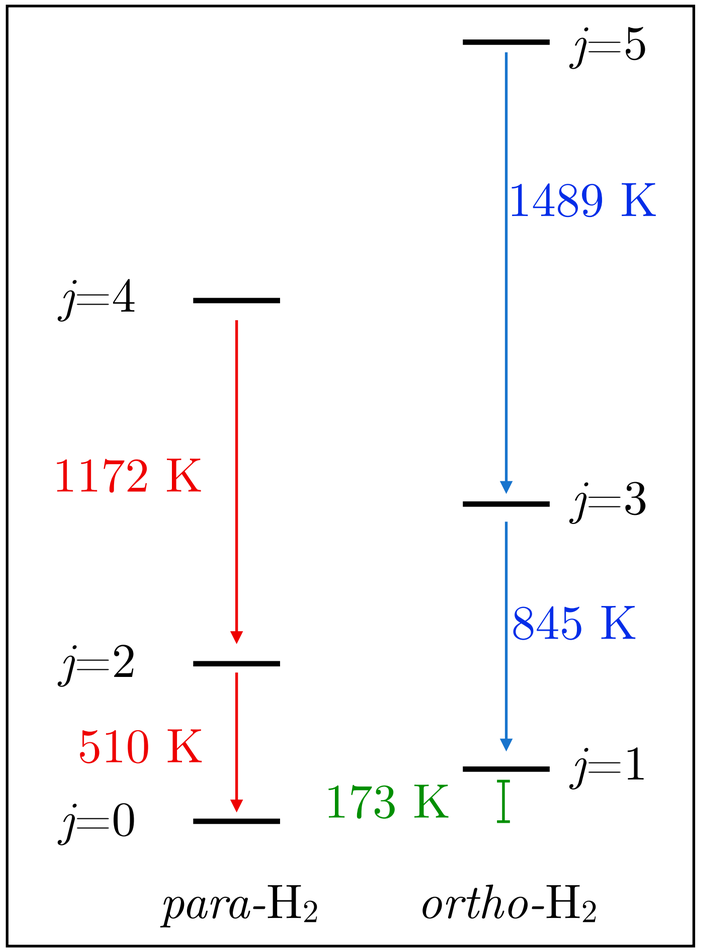

Lique+, *A&A*, **478** (2008);
Dumouchel+, *JCP*, **137** (2012).

Spherical average approximation

$j' \rightarrow j$	Cross sections / Å^2 2D	4D	% Deviation 2D/4D
$1 \rightarrow 0$	33.10	30.46	−8.68
$2 \rightarrow 0$	17.43	19.16	9.02
$3 \rightarrow 0$	9.32	8.48	−9.88
$4 \rightarrow 0$	12.64	11.89	−6.29
$5 \rightarrow 0$	11.43	11.68	2.10
$6 \rightarrow 0$	10.55	11.76	10.30
$2 \rightarrow 1$	26.61	24.55	−8.42
$3 \rightarrow 1$	16.84	15.16	−11.08
$4 \rightarrow 1$	11.75	12.82	8.38
$5 \rightarrow 1$	11.57	11.19	−3.42
$6 \rightarrow 1$	13.28	14.05	5.45
$3 \rightarrow 2$	26.06	30.57	14.73
$4 \rightarrow 2$	15.67	14.23	−10.14
$5 \rightarrow 2$	12.61	12.92	2.39
$6 \rightarrow 2$	12.77	13.55	5.76
$4 \rightarrow 3$	27.30	28.84	5.32
$5 \rightarrow 3$	14.64	14.90	1.77
$6 \rightarrow 3$	13.89	12.39	−12.11
$5 \rightarrow 4$	27.51	26.88	−2.34
$6 \rightarrow 5$	15.64	14.98	−4.44
Average absolute % deviation			7.10

PO$^+$/H$_2$ cross sections at E_{kin}=150 cm^{-1}

Tonolo+, *MNRAS*, **527** (2024).

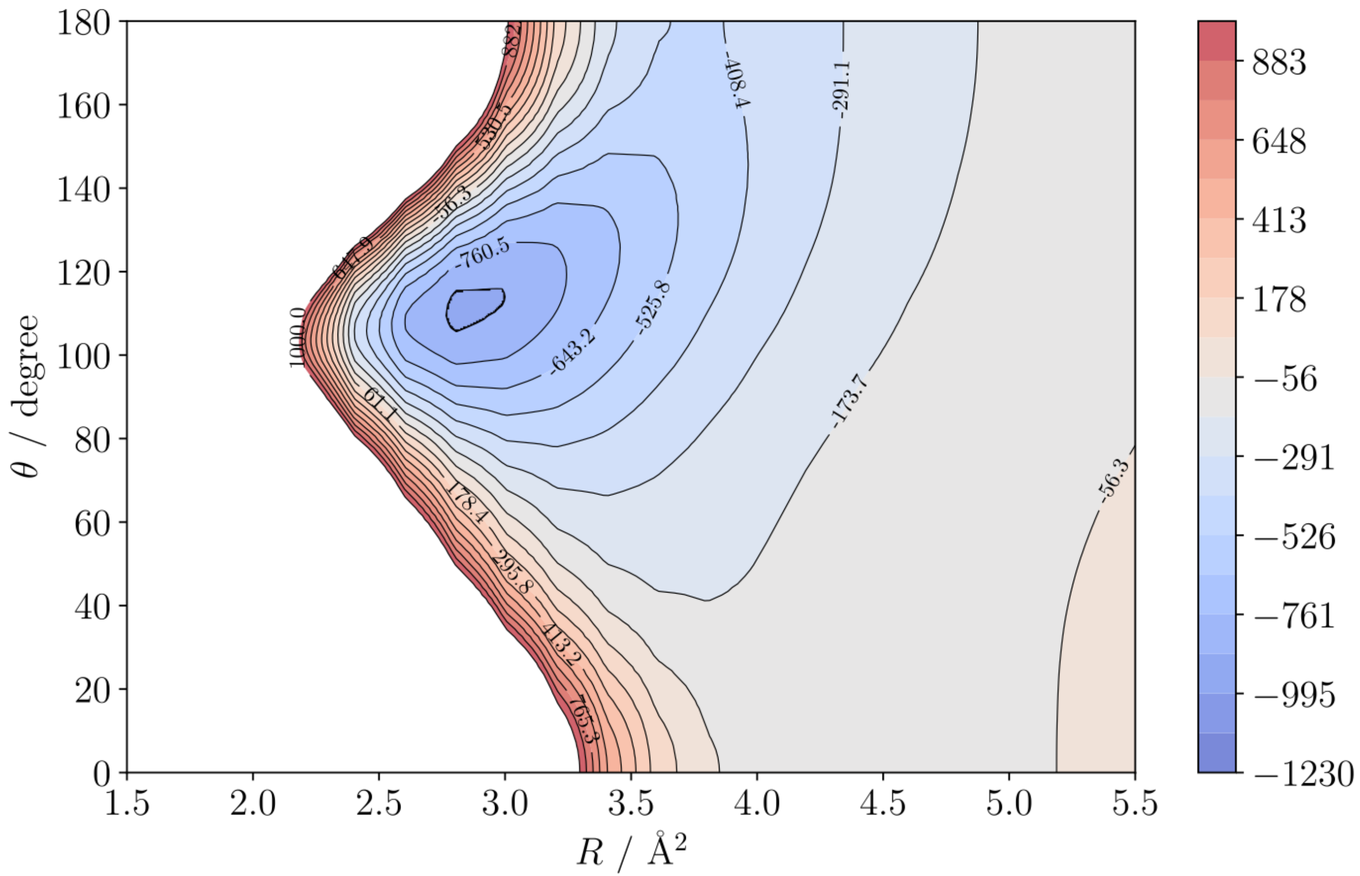

Contour plot of the averaged potential over five {θ, φ} orientations.

ortho- and para- states of the collider

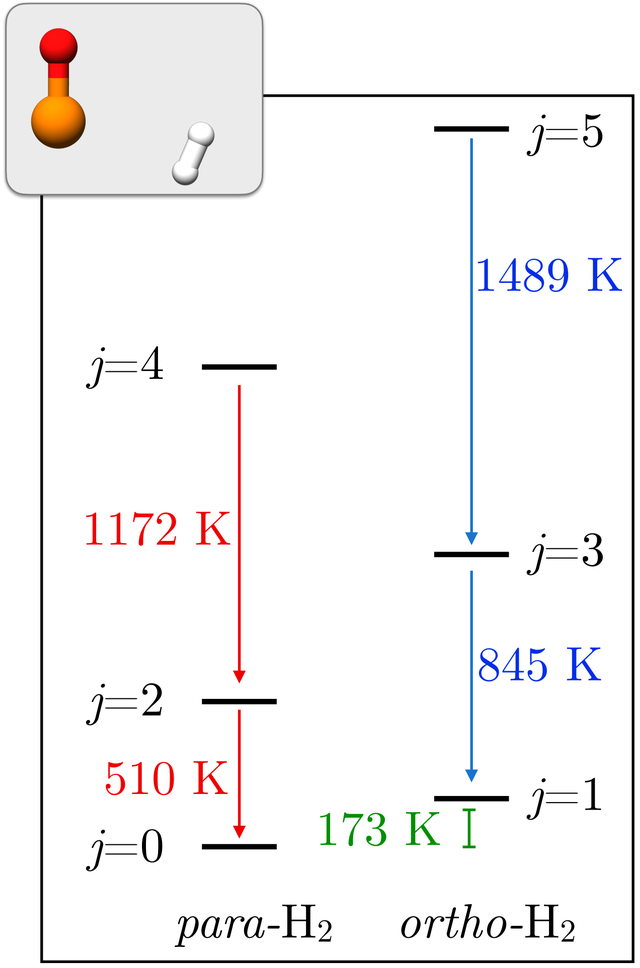

In certain circumstances, collisions with the j=1 state of the collider can also have an impact on scattering calculations.

This is the case of the G+0.693-0.027 molecular cloud where PO^+ was detected, with kinetic temperatures between 140 and 200 K.

S. Zeng, et al. (2018), *MNRAS*, **478**, 2962;
S. Zeng, et al. (2020), *MNRAS*, **497**, 4896.

Tonolo+, *MNRAS*, **527** (2024).

$j' \to j$	Cross sections / Å^2		% Deviation
	j=0	j=1	*o*-/*p*-
$1 \to 0$	33.10	33.84	−2.19
$2 \to 0$	17.43	20.46	−14.81
$3 \to 0$	9.32	10.88	−14.35
$4 \to 0$	12.64	14.39	−12.17
$5 \to 0$	11.43	12.56	−9.02
$6 \to 0$	10.55	12.26	−13.95
$2 \to 1$	26.61	29.11	−8.57
$3 \to 1$	16.84	19.70	−14.52
$4 \to 1$	11.75	13.16	−10.72
$5 \to 1$	11.57	13.92	−16.87
$6 \to 1$	13.28	17.37	−23.56
$3 \to 2$	26.06	27.96	−6.79
$4 \to 2$	15.67	18.19	−13.87
$5 \to 2$	12.61	14.26	−11.54
$6 \to 2$	12.77	17.02	−24.93
$4 \to 3$	27.30	31.06	−12.10
$5 \to 3$	14.64	16.36	−10.54
$6 \to 3$	13.89	16.93	−17.98
$5 \to 4$	27.51	29.77	−7.59
$6 \to 5$	15.64	17.08	−8.44
Average absolute % deviation			12.73

E_{kin}=150 cm^{-1}

close coupling calculations

$$\sigma_{j_B \to j'_B}(E_c) = \frac{\pi}{k^2_{j_B}} \sum_{p,J,M} \frac{2J+1}{2j_B+1} \sum_{l,l'} \left| \delta_{ll'} - S^{pJM}_{ll'} \right|^2 \longrightarrow k_{j_B \to j'_B}(T) = \left(\frac{8}{\pi \mu k_B^3 T^3} \right)^{1/2} \int_0^\infty \sigma_{j_B \to j'_B}(E_c)\, E_c \exp\left(-E_c/k_B T\right) \mathrm{d}E_c$$

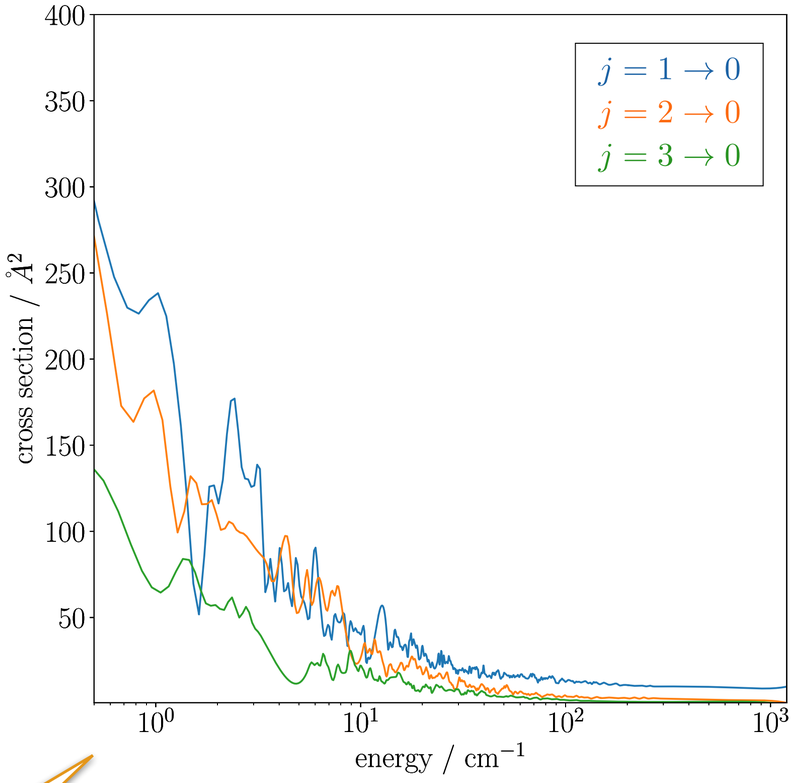

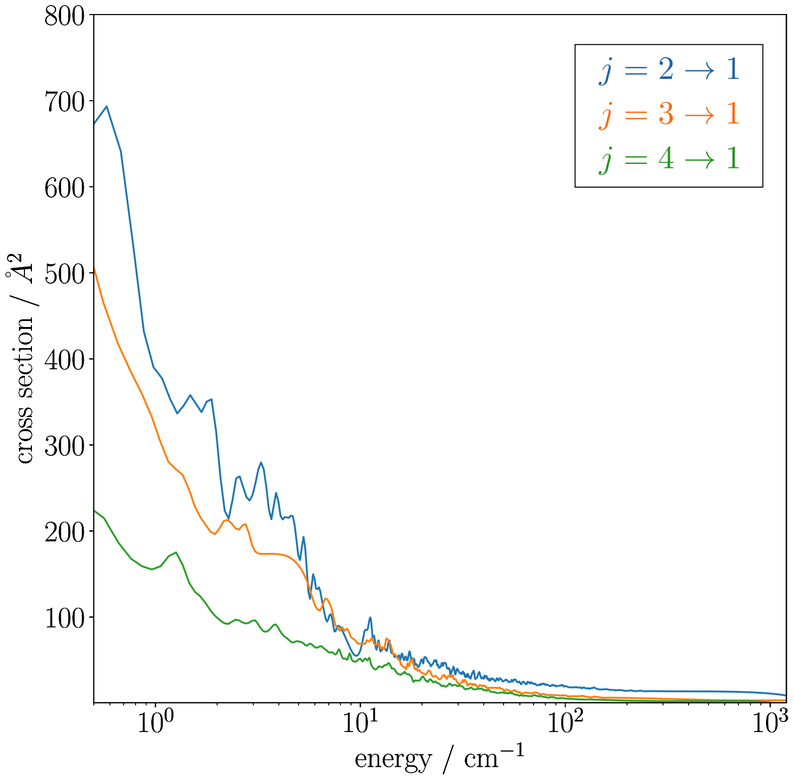

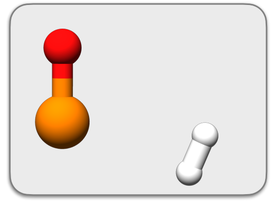

Tonolo+, *MNRAS*, **527** (2024).

close coupling calculations

$$\sigma_{j_B \to j'_B}(E_c) = \frac{\pi}{k^2_{j_B}} \sum_{p,J,M} \frac{2J+1}{2j_B+1} \sum_{l,l'} \left| \delta_{ll'} - S^{pJM}_{ll'} \right|^2 \longrightarrow k_{j_B \to j'_B}(T) = \left(\frac{8}{\pi \mu k_B^3 T^3} \right)^{1/2} \int_0^\infty \sigma_{j_B \to j'_B}(E_c)\, E_c \exp\left(-E_c/k_B T\right) \mathrm{d}E_c$$

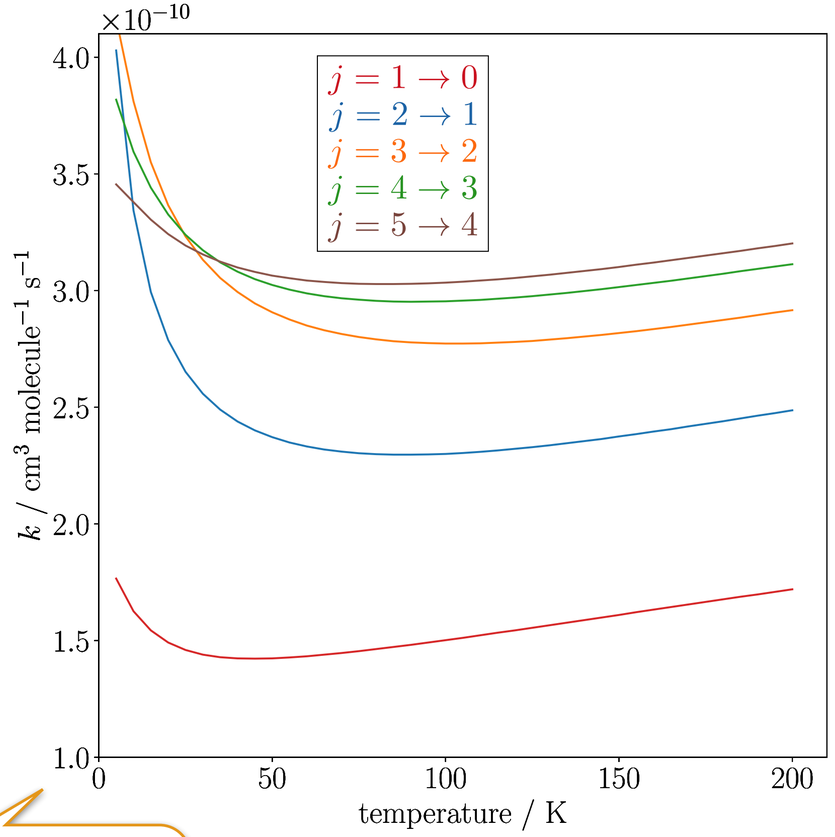

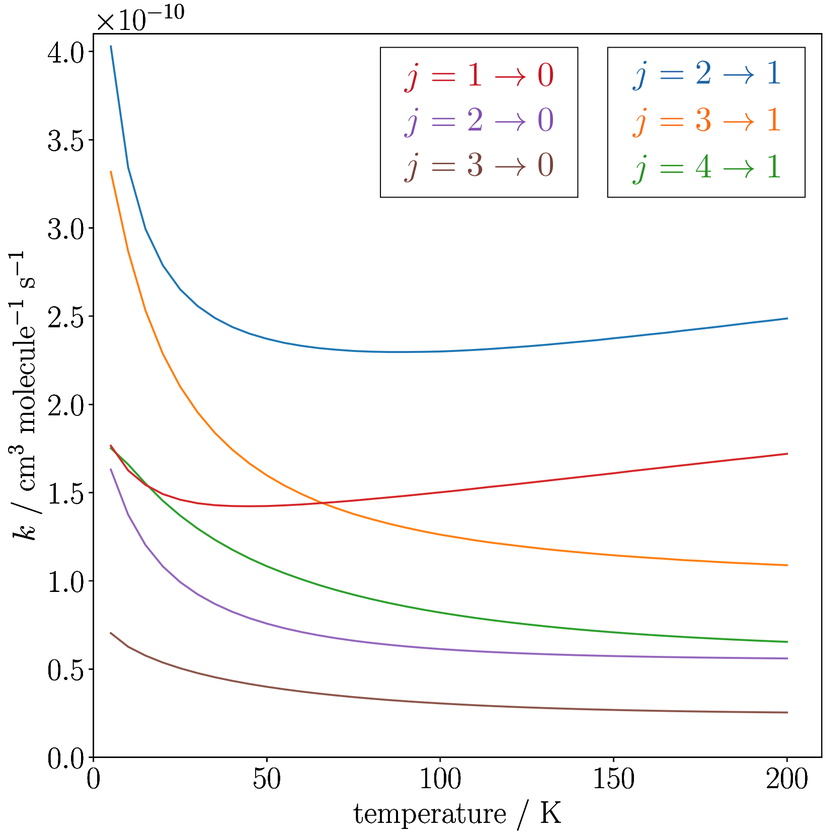

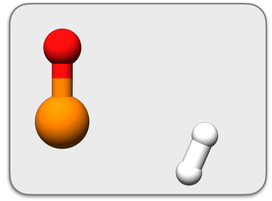

Tonolo+, *MNRAS*, **527** (2024).

close coupling calculations

$$\sigma_{j_B \to j'_B}(E_c) = \frac{\pi}{k^2_{j_B}} \sum_{p,J,M} \frac{2J+1}{2j_B+1} \sum_{l,l'} \left| \delta_{ll'} - S^{pJM}_{ll'} \right|^2 \longrightarrow k_{j_B \to j'_B}(T) = \left(\frac{8}{\pi \mu k_B^3 T^3} \right)^{1/2} \int_0^\infty \sigma_{j_B \to j'_B}(E_c)\, E_c \exp\left(-E_c/k_B T\right) \mathrm{d}E_c$$

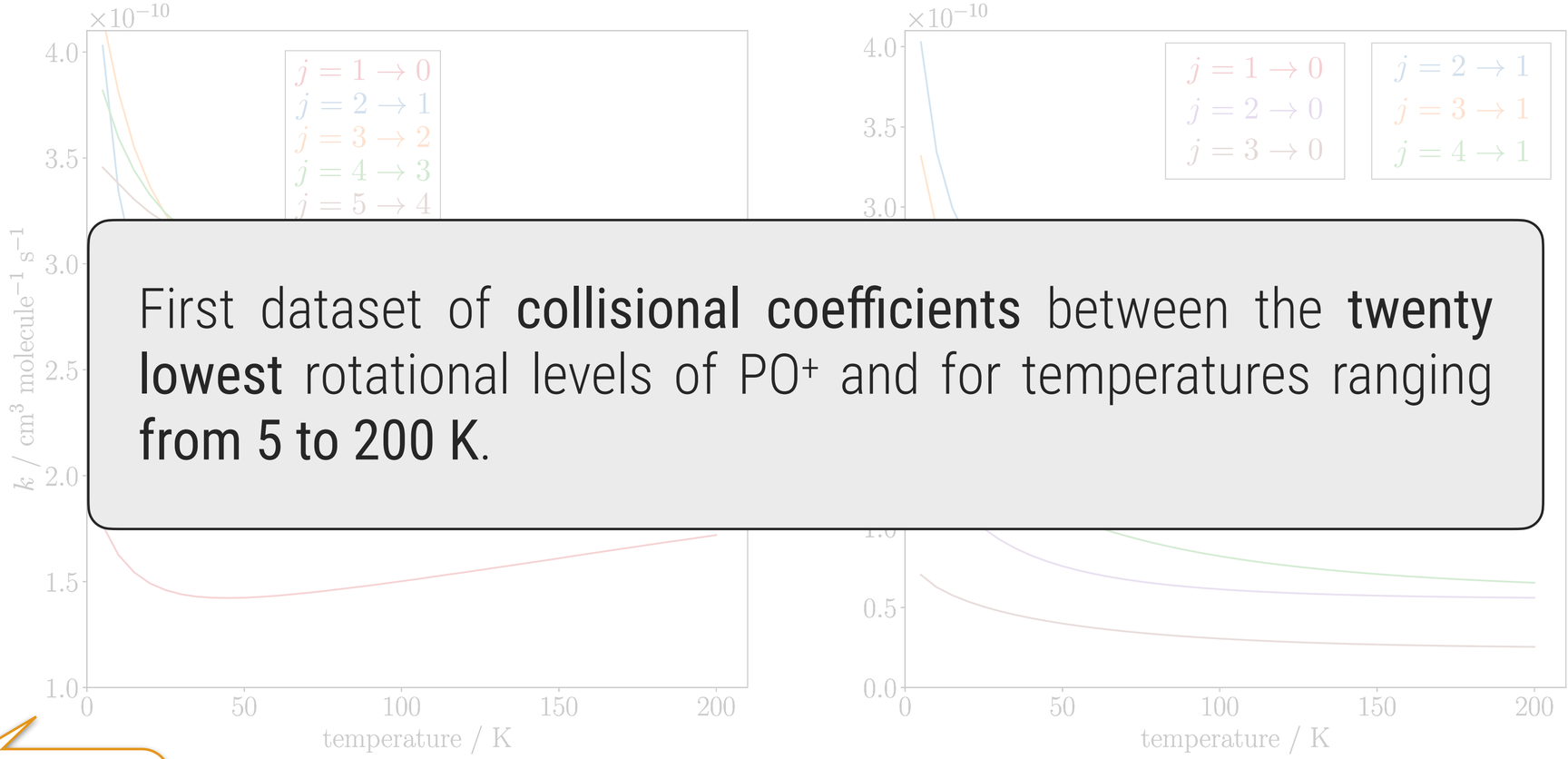

First dataset of **collisional coefficients** between the **twenty lowest** rotational levels of PO^+ and for temperatures ranging **from 5 to 200 K**.

Tonolo+, *MNRAS*, **527** (2024).

Why not using the He collider?

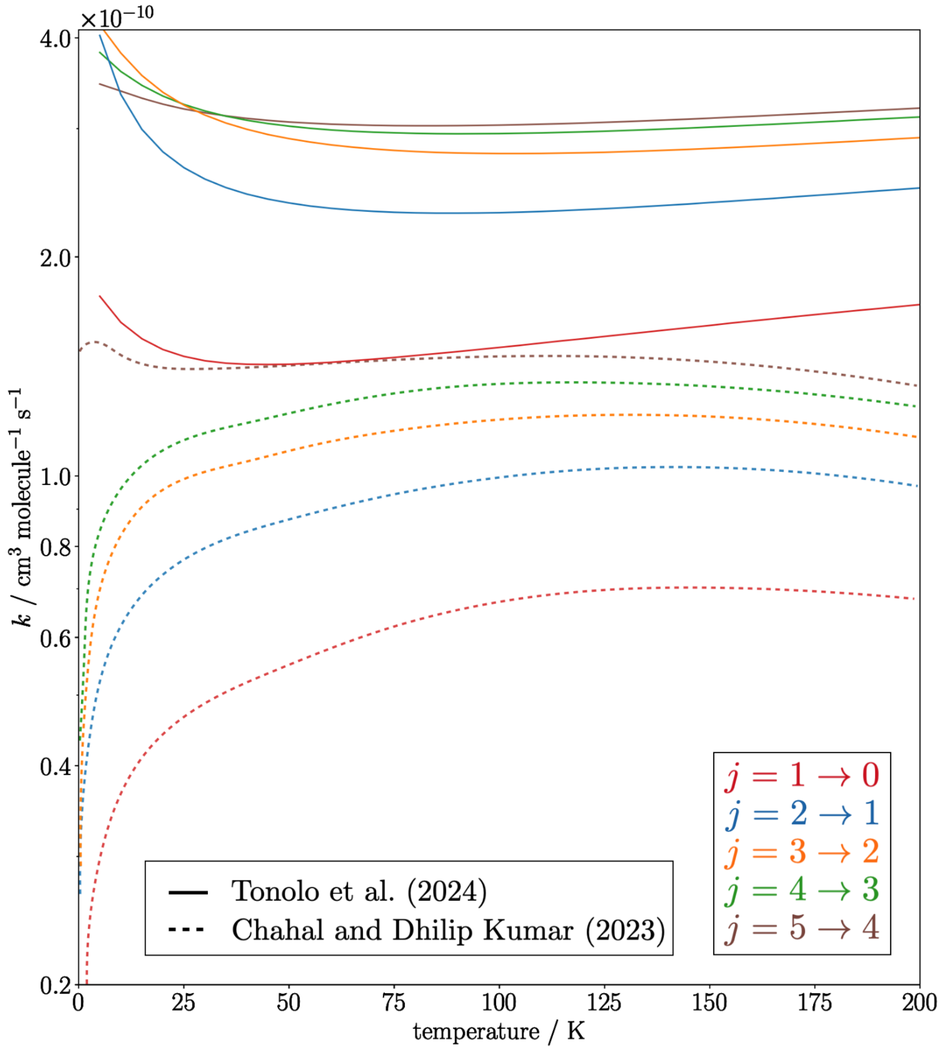

Comparison of some rotational de-excitation rate coefficients: **mass-scaled** results from previous calculations on the **PO+ and He system** (dashed lines) vs. this work (solid lines).

↓

Inaccuracy of He as a proxy of the H_2 perturber!

Tonolo+, *MNRAS*, **527** (2024);
Chalal+, *MNRAS*, **523** (2023).

Radiative transfer modeling

The recent detection of PO^+ in the **molecular cloud G+0.693-0.02** where, due to the low density of H_2, **LTE condition are not achieved**, motivated the need of collisional rate coefficients to properly model its abundance.

V. M. Rivilla, et al. (2022), *FSPAS*, **9**, 829288.

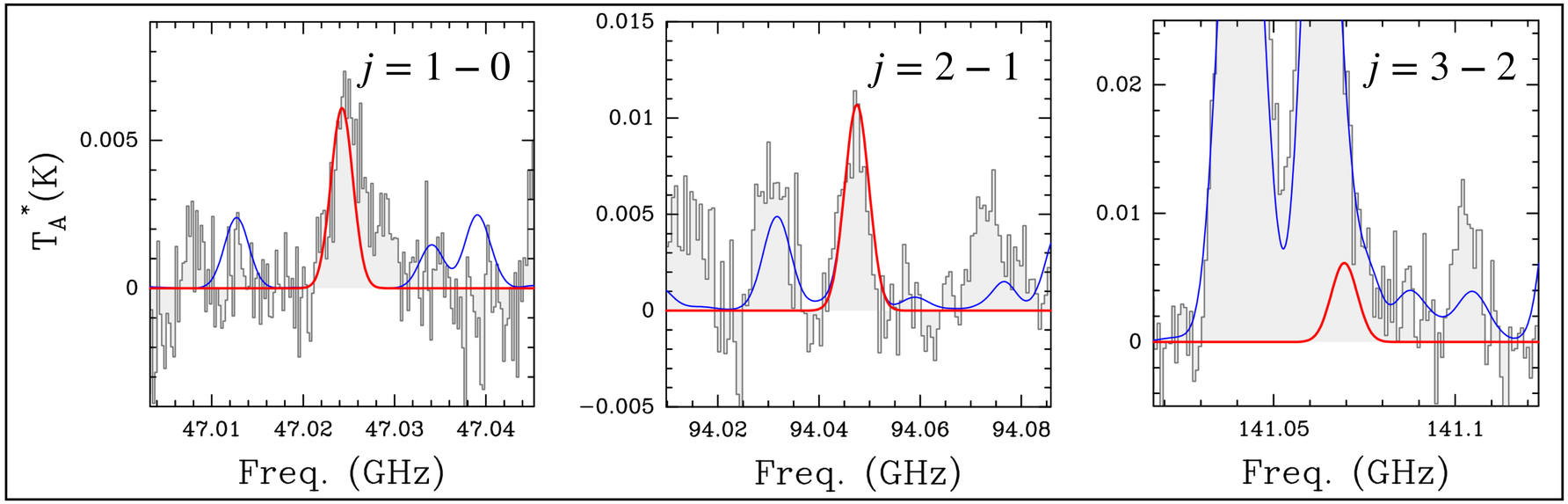

G+0.693-0.027 molecular cloud:

- Very low densities of H_2 ($\sim 1 \times 10^4$ cm^{-3});
- High kinetic temperatures (~ 150 K);

$\longrightarrow$ Quasi-thermalization condition!

$$T_{ex} \sim 5 - 20\,K$$

S. Zeng, et al. (2018), *MNRAS*, **478**, 2962;
S. Zeng, et al. (2020), *MNRAS*, **497**, 4896.

P. F. Goldsmith and W. D. Langer (1999), *ApJ*, **517**, 209.

Radiative transfer modeling

RADEX

Radiative transfer calculations have been used to model the observation of PO^+ in G+0.693-0.027.

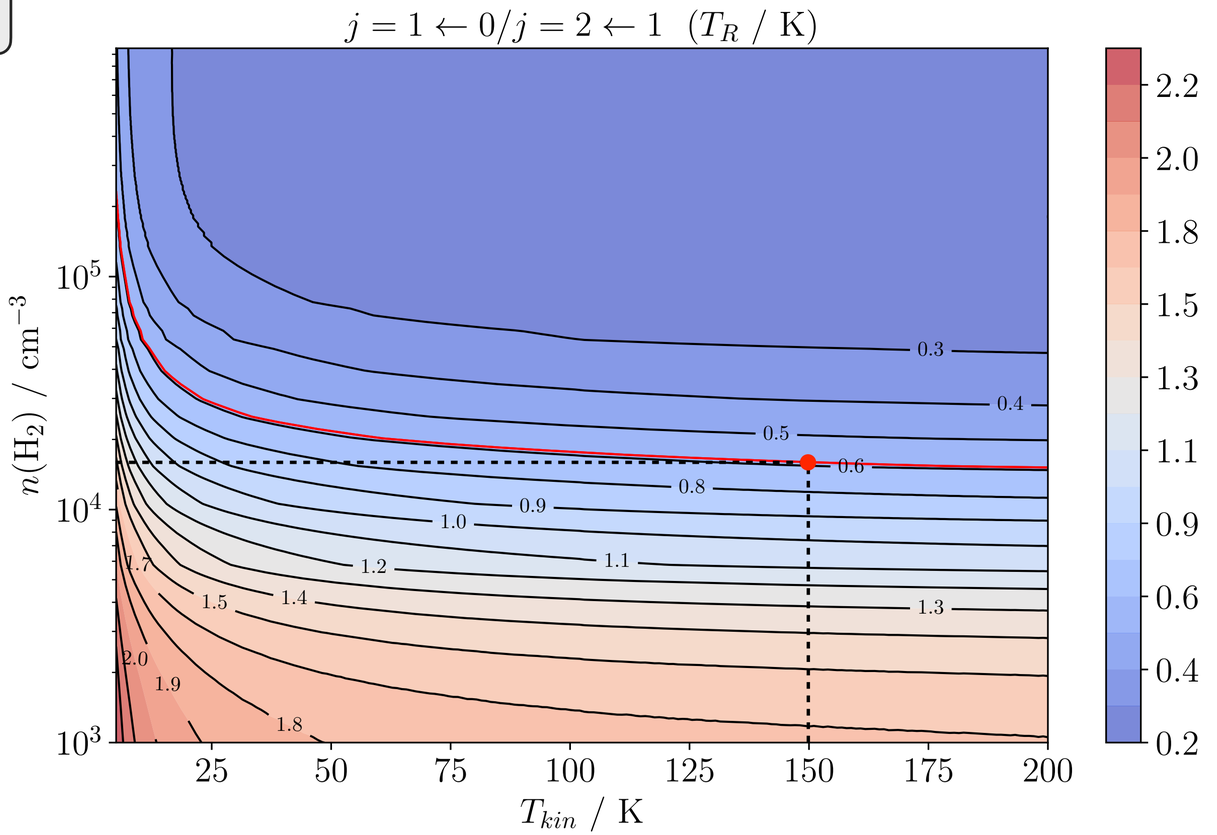

$$n(H_2) \sim 1.5 \times 10^4 \,\mathrm{cm}^{-3}$$

Variation of the j=1-0/j=2-1 intensity ratio as a function of T_{kin} and $n(H_2)$. The observed intensity ratio is highlighted in red.

Radiative transfer modeling

Single transition analysis: intensity trends at 150 *K* as a function of $n(H_2)$ and *N*.

RADEX

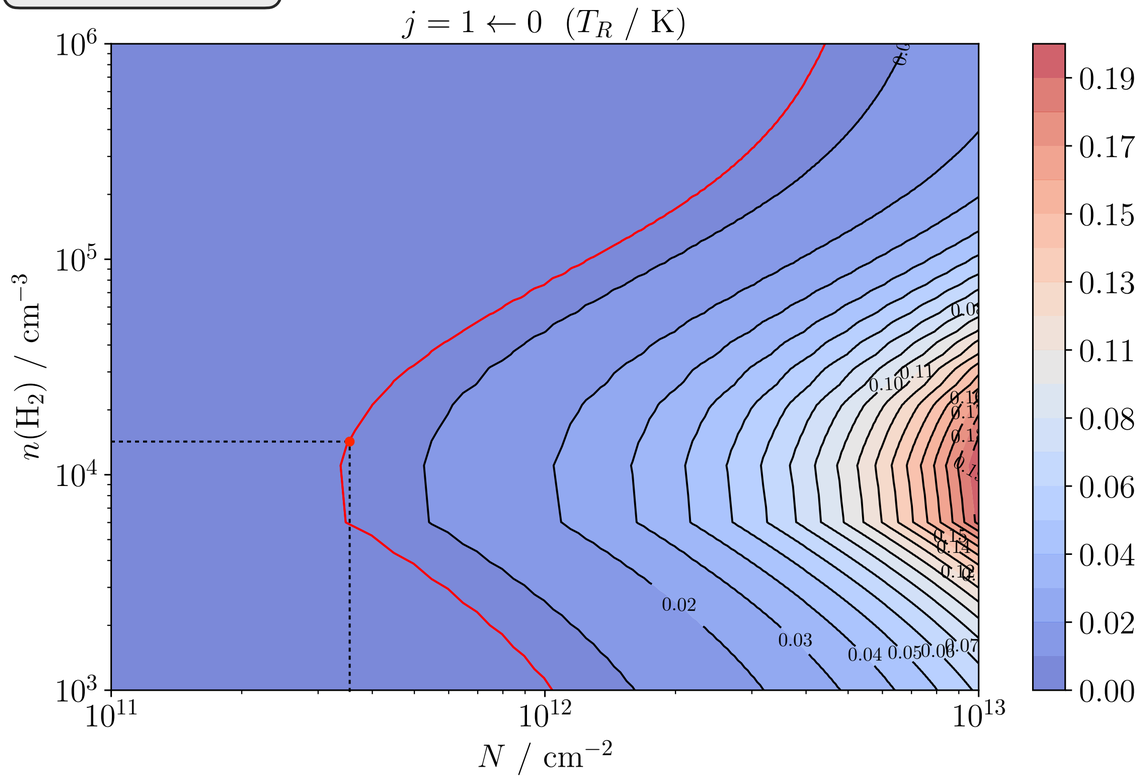

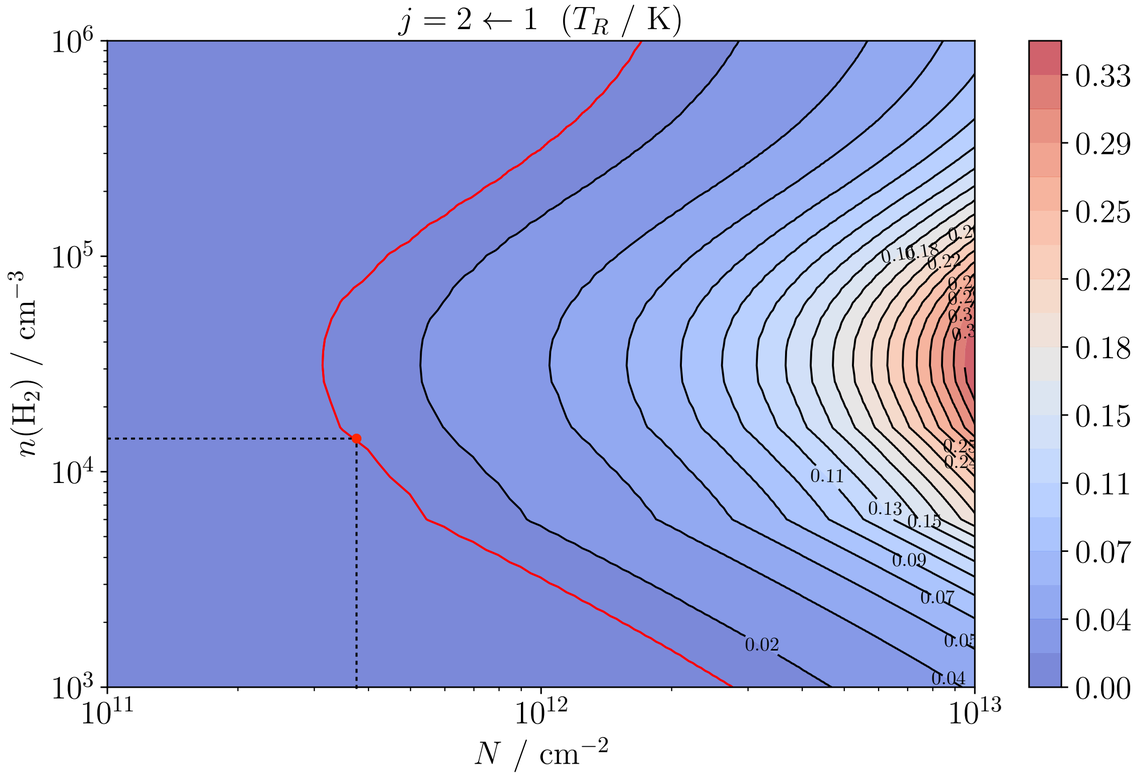

$N \sim 3.7 \times 10^{11}\,\mathrm{cm}^{-2}$ → A factor of ~60% smaller than the previously LTE-derived value.

Radiative transfer modeling

RADEX

Behavior of T_{ex} for j=1-0 and j=2-1 at different densities and temperature conditions —> For densities around 10^5 cm^{-3}, **maser phenomena** are predicted.

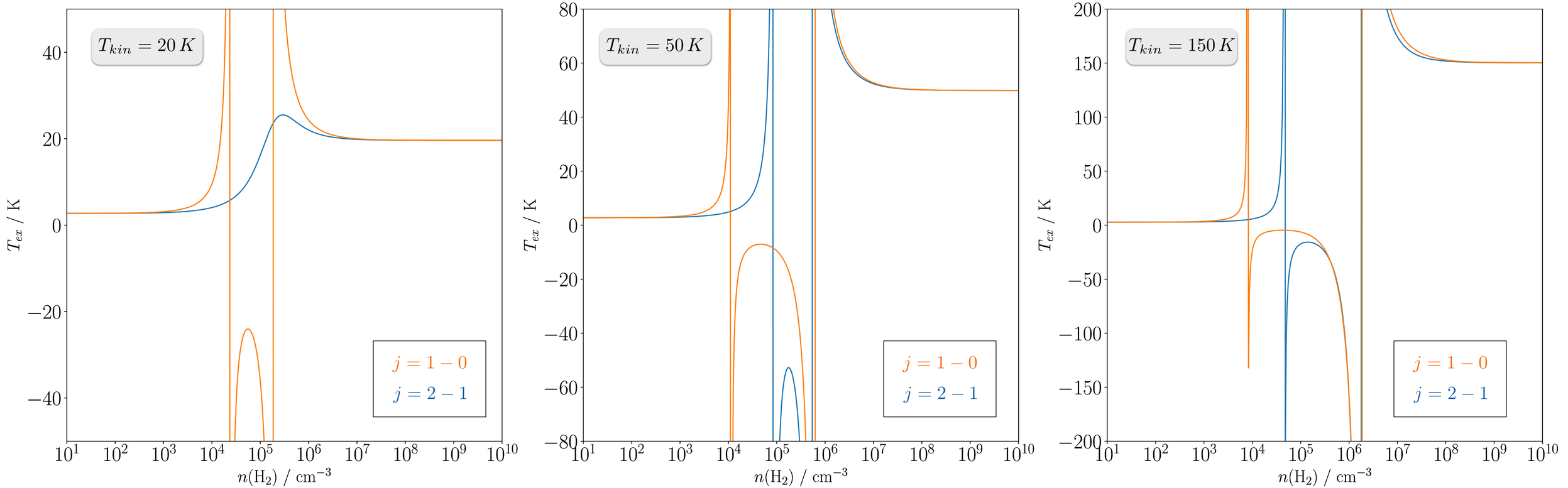

Variation of the excitation temperature as a function of n(H_2) for the first two transitions of PO^+ at T_{kin}=20, 50, 150 K.

Tonolo+, *MNRAS*, **527** (2024).

Conclusions

PO^+ and H_2 collisional system

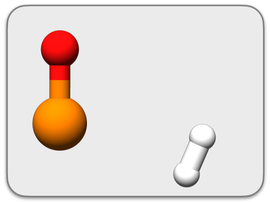

Characterization of the Interaction Potential

Single point energies at **CCSD(T)-F12/aug-cc-pV(Q+d)Z** level of theory + **spherical average approximation** to fit the potential.

Scattering Calculations

First dataset of **collisional coefficients** between the **twenty lowest** rotational levels of PO^+ and for temperatures ranging **from 5 to 200 K**.

Astrophysical Modeling

Radiative transfer modeling of the recently observed lines that allowed to **refine the abundance of PO^+** measured in the G+0.693−0.027 cloud. Strong **maser effects** highlight the importance of collisional data for astrophysical applications.

Thank you!

Prof. François Lique

Prof. Cristina Puzzarini
Dr. Luca Bizzocchi
Dr. Mattia Melosso

ALMA MATER STUDIORUM
UNIVERSITÀ DI BOLOGNA

Dr. Victor M. Rivilla

CENTRO DE ASTROBIOLOGÍA · CAB
ASOCIADO AL NASA ASTROBIOLOGY PROGRAM
CSIC INTA

COLLEXISM

European Research Council
Established by the European Commission